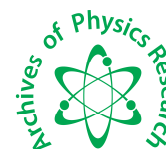




## Scholars Research Library

Archives of Physics Research, 2014, 5 (1):18-24  
(<http://scholarsresearchlibrary.com/archive.html>)



Scholars Research  
Library

ISSN : 0976-0970

CODEN (USA): APRRC7

### Synthesis of magnesium-zinc nano ferrites by using Aloe vera extract solution and their structural and magnetic characterizations

Sanjay Kumar<sup>\*1</sup>, Ashwani Sharma<sup>1</sup>, Mahabir Singh<sup>2</sup> and Satya Prakash Sharma<sup>3</sup>

<sup>1</sup>Department of Physics, M. D. University, Rohtak, India

<sup>2</sup>Department of Physics, H. P. University, Shimla, India

<sup>3</sup>Department of Chemistry, Shri Baba Mast Nath University, Rohtak, India

---

#### ABSTRACT

$Mg_x Zn_{1-x} Fe_2 O_4$  ( $x = 0.25, 0.45$ ) ferrite nanoparticles were prepared by a modified sol-gel method using high purity metal nitrates and aloe vera plant extracted solution. Using of aloe vera extract simplifies the process, provide an alternative process for a simple and economical synthesis of nanocrystalline ferrite. The structural characteristics of calcined sample of  $Mg_x Zn_{1-x} Fe_2 O_4$  ( $x = 0.25, 0.45$ ) ferrite nanoparticles were determined by X-ray diffraction (XRD), Fourier transform infrared spectroscopy (FT-IR) and transmission electron microscopy (TEM). The prepared samples have spinel structure. From XRD we observed that particle size decreases with increasing Mg content. Nano size of the particles was confirmed by TEM measurement. Magnetization measurements were obtained at room temperature by using Vibrating sample magnetometer (VSM), which showed that the calcinated samples exhibited super paramagnetic behaviour.

**Keywords:** Sol-gel, Aloe-vera, Synthesis, Magnetic properties, Electron microscopy, Spinel

---

#### INTRODUCTION

ferrites are mostly used as various inductance components, such as magnetic cores of filters, transformers, deflection, antenna, video magnetic heads and magnetic heads of multiple path communication and so on. Furthermore, the material has also brought potential applications in magnetic liquid absorbing materials [1-7]. With rapid development of electronic information industries such as communications and computer networks, the size of electronic apparatus and equipments is miniaturized [8-9]. Demand for electronic components with high density, light weight, thin type and fine performance is greatly increasing, which accelerate the demand for soft magnetic ferrites with high performance and thus contributes to the development of soft magnetic ferrites on the direction of higher frequency and lower power consumption [10-15]. Ferrite particles in nano scales can be produced by soft chemical methods, such as co-precipitation, sol-gel and hydrothermal synthesis [16-17]. Among other established synthesis methods, simple and cost effective routes to synthesize nanocrystalline Mg-Zn ferrite by utilization of cheap, non-toxic and environmentally benign precursors are still the key issue.

Chandran et al. have demonstrated the synthesis of nanotriangle gold and nanosilver using aloe vera plant extracts as a reducing agent. In this work, the sizes of nanotriangle gold were about 50-350 nm and nanosilver were about 5-15 nm [18-20]. In this present work, we report for the synthesis of nanoparticles of Mg-Zn ferrite by simple method using metal nitrates and aloe vera extract solution as a precursors. The samples were characterized by, XRD, FT-IR

and TEM. The magnetic properties of prepared nanoparticles were investigated by vibrating sample magnetometer (VSM).

## MATERIALS AND METHODS

### 1.1. Materials

All materials were of analytical grade and were used without further purification. Distilled water was used in all experiments.

### 1.2. Synthesis of $Mg_x Zn_{1-x} Fe_2 O_4$ ferrite nanoparticles

In this study, the  $Mg_x Zn_{1-x} Fe_2 O_4$  ferrite nanoparticles was synthesized by the modified sol-gel method. In this study either  $Zn(NO_3)_2 \cdot 6H_2O$  or  $Mg(NO_3)_2 \cdot 6H_2O$  mixed with  $Fe(NO_3)_3 \cdot 9H_2O$  were used as the starting materials. In a typical procedure, 60 ml of aloe vera plant extract, instead of toxic organic polymers, was mixed with 40 ml distilled water under vigorous stir until homogenous solution was obtained. According to this formula  $Mg_x Zn_{1-x} Fe_2 O_4$  ( $x = 0.25, 0.45$ ), each metal nitrate was added slowly to the aloe vera solution under vigorous stirring for 2 h to obtain a well – dissolved solution. No pH adjustment was made. Then the, the mixed solution was evaporated by heating on the hot plate at  $100^\circ C$  under vigorous stirring for several hours until a dried precursor was obtained. The dried precursor was crushed into powder using mortar and pestle. The dried precursor then was calcinated in a muffle – furnace at  $700^\circ C$  for 2 h.

### 1.3. Particle characterization

The X- ray diffraction (XRD) patterns of the samples were recorded on a PANalytical X'Pert PRO X-ray diffractometer using  $Cu K\alpha$  radiation ( $\lambda = 0.15406 \text{ \AA}$ ). The crystallite size of nanocrystalline samples was measured from the line broadening analyses using Debye-Scherrer formula after accounting for instrumental broadening (Equation 1):

$$D_{XRD} = 0.89 \lambda / \beta \cos \theta \quad (1)$$

Where  $\lambda$  – wavelength of X-ray radiation used in  $\text{\AA}$ ,  $\theta$  is the diffraction angle,  $\beta$  is the full width at half maximum (FWHM) in radians in the  $2\theta$  scale,  $D_{XRD}$  is the crystallite size in nm [22].

### 1.4. Particle Morphology

The particle morphology was examined by transmission electron microscopy (HITACHI model H-7500). For the TEM observations, powders were supported on carbon-coated copper grids which was ultrasonically dispersed in ethanol.

### 1.5. Magnetic measurements

Room temperature magnetic measurements were carried out using a Lakeshore vibrating sample magnetometer (VSM) and parameters like specific saturation magnetization (Ms), coercive force (Hc) and remanence (Mr) were evaluated.

### 1.6. Spectral measurements

FTIR spectra were recorded for dried samples of  $Mg_x Zn_{1-x} Fe_2 O_4$  ( $x = 0.25, 0.45$ ) with an Perkin – Elmer FTIR spectrometer. The dried samples were in KBr matrix, and spectra were measured according to transmittance method.

## RESULTS AND DISCUSSION

### 2.1. XRD Analysis

Generally, XRD can be used to characterize the crystallinity of nanoparticles. It gives the average diameters of all the nanoparticles. The fine particles were characterized by XRD for structural determination and estimation of crystallite size. XRD pattern were analyzed. All experimental peaks were matched with theoretically generated one and indexed. The XRD patterns of all the samples were shown in Fig.1.

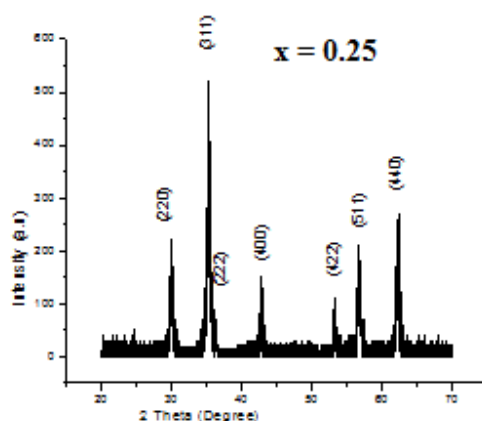


Fig. 1(a) XRD patterns of  $Mg_{0.25}Zn_{0.75}Fe_2O_4$  ferrites nanoparticles calcinated at  $700^{\circ}C$  for 2 h

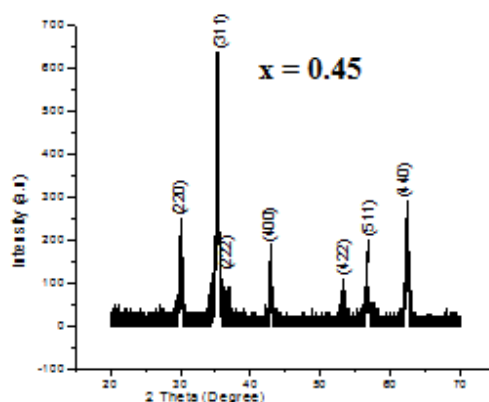


Figure.1(b)

Fig. 1(b) XRD patterns of  $Mg_{0.45}Zn_{0.55}Fe_2O_4$  ferrites nanoparticles calcinated at  $700^{\circ}C$  for 2h

It shows the formation of spinel ferrite phase in all the samples. The broad XRD line indicates that the ferrite particles are in nano size. The crystallite size for each composition are calculated from XRD line width of the (311) peak using Scherrer formula [21]. The average crystallite size decreases from 23.8 nm to 23.0 nm when the partial substitution of Mg increases. Both samples were prepared under identical condition. The crystallite size was not the same for all the Mg concentrations. This was probably due to the preparation condition followed here which gave rise to different rate of ferrite formation for different concentrations of Mg, favoring the variation of crystallite size. The values of the particle size, lattice constant and unit cell volume as deduced from X-ray data are given by Table 1. The lattice constant was found to decrease from 8.371 to 8.82 Å with increase in Mg concentration as shown in Table 1.

Table 1. Crystallite size, Lattice constant and unit cell volume for  $Mg_xZn_{1-x}Fe_2O_4$  ( $x=0.25, 0.45$ ) nanoferrites calcinated at  $700^{\circ}C$  for 2h

Nickel Concentration(x)	Crystallite Size (D) (nm)	Lattice constant (Å)	Unit Cell Volume $a^3$ ( Å <sup>3</sup> )
0.25	23.8	8.382	588.901
0.45	23.0	8.371	586.586

The strongest reflection comes from the ( 311 ) plane. Which denotes the spinel phase. All the compositions had a spinel structure. The peaks indexed to (200), ( 311 ), ( 400 ), ( 422 ), ( 511 ) and ( 440 ) planes of a cubic unit cell, corresponds to cubic spinel structure. The calculated lattice constant (Å), identified the sample to be cubic spinel.

## 2.2. Transmission electron microscopy

The morphology and structure of the prepared ferrite samples calcinated at  $700^{\circ}C$  for 2 hours were investigated by TEM techniques as shown in Fig. 2. The results indicate that the samples prepared by sol-gel method are almost uniform in both morphology and particle size distribution. A close inspection would reveal the presence of particles

showing the spherical in shape. The particle sizes increased with increasing Mg concentration. Mean particle size from TEM image is in good agreement with the crystallite size measured from X-ray line (311) broadening using Scherrer's formula. This is lower than the particle size of nanoferrites prepared by other chemical method [15].

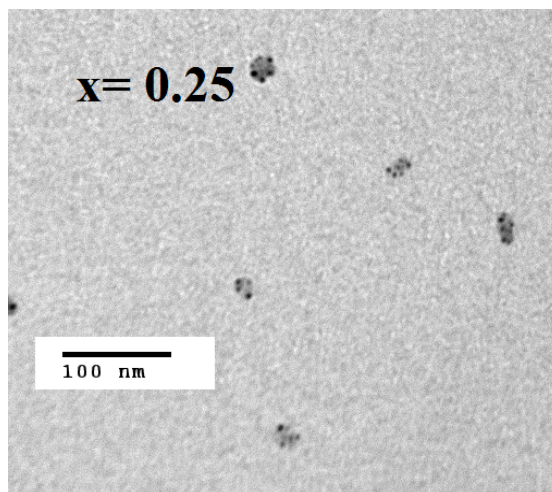


Figure 2(a) TEM images of  $\text{Mg}_{0.25}\text{Zn}_{0.75}\text{Fe}_2\text{O}_4$  ferrites nanoparticles calcinated at  $700^\circ\text{C}$  for 2h

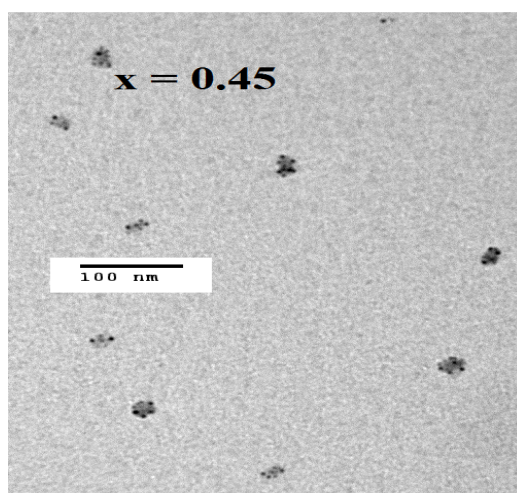


Figure 2(b) TEM images of  $\text{Mg}_{0.45}\text{Zn}_{0.55}\text{Fe}_2\text{O}_4$  ferrites nanoparticles calcinated at  $700^\circ\text{C}$  for 2h

### 2.3. Fourier transform infrared analysis ( FT-IR ) measurements

FTIR spectral analysis helps to confirm the formation of spinel structure in ferrite samples. The FTIR spectra of the investigated  $\text{Mg}_x\text{Zn}_{1-x}\text{Fe}_2\text{O}_4$  ( $x = 0.25, 0.45$ ) samples are shown in figure 3. In the wave number range of  $1000\text{--}300\text{ cm}^{-1}$ , two main broad metal–oxygen bands are seen in the infrared spectra of all spinels, especially ferrites. The higher one ( $\nu_1$ ) generally observed in the range  $600\text{--}550\text{ cm}^{-1}$ , is caused by the stretching vibrations of the tetrahedral metal–oxygen bond. The lowest band ( $\nu_2$ ) usually observed in the range  $450\text{--}440\text{ cm}^{-1}$ , is caused by the metal–oxygen vibrations in the octahedral sites (Waldron 1955). This difference in the spectral positions is expected because of the difference in the  $\text{Fe}^{3+}\text{--O}^{2-}$  distance for the octahedral and tetrahedral compounds. This is confirmed from Fourier transform Infrared spectroscopy ( FTIR) that the structure remains cubic spinel after magnesium substitution in zinc nano ferrite [22-24]. The vibrational frequencies of IR bands  $\nu_1$  and  $\nu_2$  of samples prepared by sol–gel are shown in figure 3, which are in perfect agreement with reported values (Montemayor et al 2007; Priyadharsini et al 2009. technique, annealed at  $400^\circ\text{C}$ ). The spectra show prominent bands near  $3400$  and  $1600\text{ cm}^{-1}$ , which are attributed to the stretching modes and H–O–H bending vibrations of the free or absorbed water. The peaks are around  $3429.27\text{ cm}^{-1}$ ,  $2921\text{ cm}^{-1}$ , corresponding to the stretching and bending vibration of O-H, C-H.

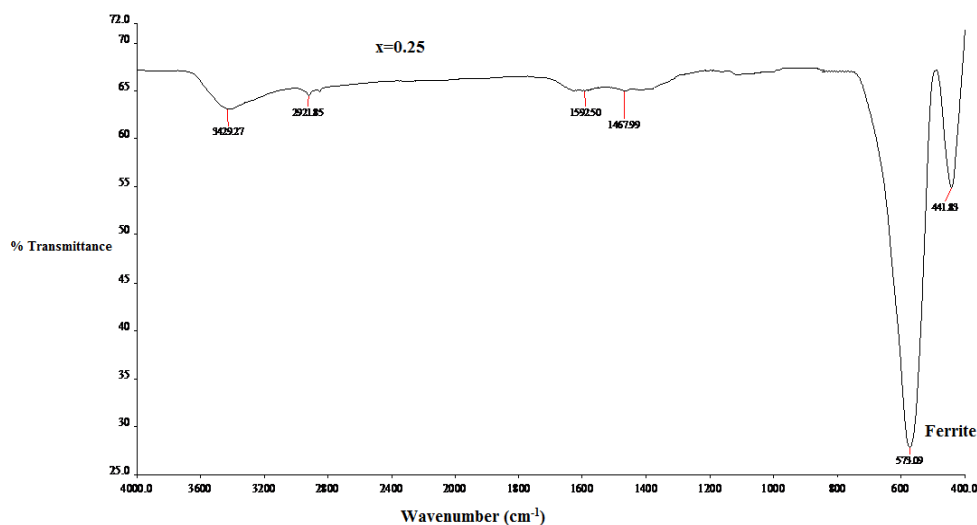


Figure 3(a) FTIR spectrographs of  $\text{Mg}_{0.25}\text{Zn}_{0.75}\text{Fe}_2\text{O}_4$  ferrites nanoparticles calcinated at  $700^\circ\text{C}$  for 2h

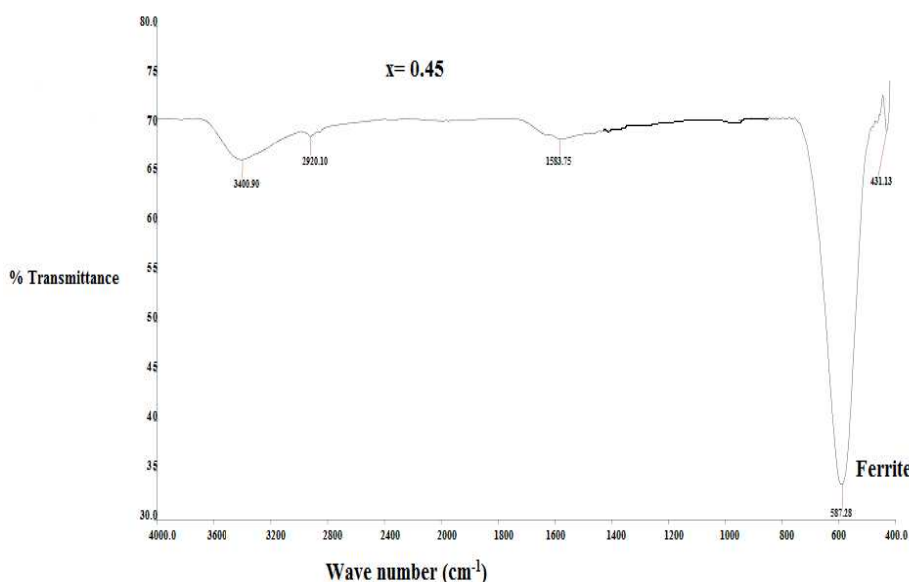
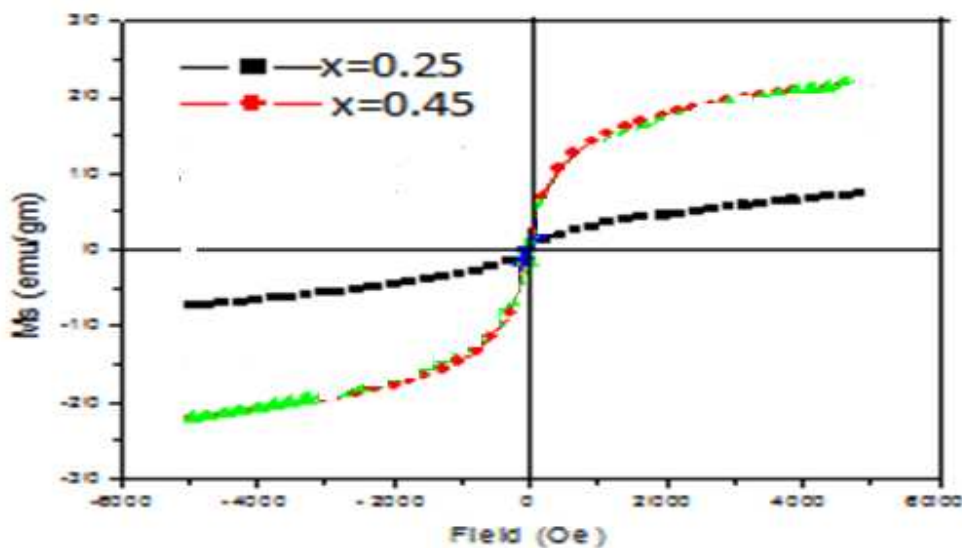


Figure 3(b) FTIR spectrographs of  $\text{Mg}_{0.45}\text{Zn}_{0.55}\text{Fe}_2\text{O}_4$  ferrites nanoparticles calcinated at  $700^\circ\text{C}$  for 2h

#### 2.4. Magnetic measurements

From the hysteresis curve one can get information such as saturation magnetization ( $M_s$ ), coercivity ( $H_c$ ), remanance magnetization ( $M_r$ ) and squareness ratio ( $M_r/M_s$ ) for a given sample. The magnetic properties of the  $\text{Mg}_x\text{Zn}_{1-x}\text{Fe}_2\text{O}_4$  ( $x=0.25, 0.45$ ) nanoferrites powder sample can be determined at room temperature using Vibrating Sample magnetometer (VSM) with applied field up to 6000Oe. Figure 4 shows the variation of magnetization with applied field for all four  $\text{Mg}_x\text{Zn}_{1-x}\text{Fe}_2\text{O}_4$  ( $x=0.25, 0.45, \dots$ ) nanoferrites. The hysteresis curve (Figure 4) recorded at room temperature shows very low coercivity, remanence at room temperature. Nanoferrites do not attain saturation in applied field. From table 4.6 the reduced values of the  $M_r/M_s$  ratio shows a powder ferrite behaviour, within the magnetization field, closer to the superparamagnetic one.



**Figure 4.** Variation of magnetization with applied field at room temperature for  $Mg_{0.25}Zn_{0.75}Fe_2O_4$  and  $Mg_{0.45}Zn_{0.55}Fe_2O_4$  ferrites nanoparticles

Among studied ferrites  $Mg_{0.45}Zn_{0.55}Fe_2O_4$  has the highest specific magnetization. It is known that magnetization in ferrites proceeds through the movement of the domain walls and domain rotations and the coercive force is obtained by reversal of the directions of the wall movement and that of the domain rotation. The larger the particle size, the greater the probability of domain formation and domain rotation [25-27]. On other hand, the smaller the particles contain less domain walls and require higher force for demagnetization [28]. Calculated values of Saturation Magnetization (Ms), Coercivity (Hc), Remanent Magnetization (Mr) and Squareness ratio for  $Mg_x Zn_{1-x} Fe_2O_4$  ( $x=0.25, 0.45$ ) nanoferrites at  $700^\circ C$  for 2 hours. Calculated values of Saturation Magnetization (Ms), Coercivity (Hc), Remanent Magnetization (Mr) and Squareness ratio for  $Mg_x Zn_{1-x} Fe_2O_4$  ( $x=0.25, 0.45$ ) nanoferrites at  $700^\circ C$  for 2 hours as shown in table 2.

**Table 2.** Calculated values of Saturation Magnetization (Ms), Coercivity (Hc), Remanent Magnetization (Mr) and Squareness ratio for  $Mg_x Zn_{1-x} Fe_2O_4$  ( $x=0.25, 0.45$ ) nanoferrites at  $700^\circ C$  for 2 hours

Ni concentration (x)	Magnetic Properties			
	Saturation Magnetization (Ms)(emu/gm)	Coercivity (Hc) (Oe)	Remanent Magnetization (Mr)(emu/gm)	Squareness Ratio (R= Mr/Ms)
0.25	07.37	26.65	0.39	0.05
0.45	21.9	29.32	2.27	0.10

## CONCLUSION

$Mg_x Zn_{1-x} Fe_2O_4$  ( $x=0.25, 0.45$ ) nanoferrites with varying x were synthesized by a simple solution route using high purity nitrates and aloe vera plant extract solution. From XRD, FT-IR spectra and TEM analysis, it is indicated that the crystalline spinel ferrite can be obtained using calcination temperature at  $700^\circ C$  for 2h. XRD pattern confirms the synthesis of fully crystalline single phase Mg-Zn nano ferrites. The particle size size of nanocrystalline spinel ferrite calculated from FWHM of XRD (311) peak and in good agreement with TEM result. The reduced values of the Mr/Ms ratio shows a powder ferrite behaviour, within the magnetization field, closer to the superparamagnetic one.

This work demonstrates the use of a simple synthetic method using cheap precursors of Aloe vera plant extract provides high – yield nanosized ferrites with well crystalline structure and uniform particle sizes, energy saving, high purity, no reaction with containers which increases purity, no pH adjustment, environmental friendly, and acceptable magnetic properties.

**Acknowledgements**

Author is grateful to SAIF Punjab University, Chandigarh for characterization (XRD, TEM and FTIR ) and to National Physical Laboratory, Delhi for VSM measurement.

**REFERENCES**

- [1] M K Titulaer , J B H Jansen and J W Geus . *Clays Clay Miner.* **1994**,42,249 .
- [2] M S Cao , H T Liu, Y J Chen , B Wang and Zhu *J. Sci. Chin. E.* **2003**, 46, 104
- [3] M S Cao, R G Wang , X Y Fang , Z X Cui, T J Chang and H J Yang . *Powder Technol.* **2001**, 115, 1293
- [4] J M Wang, Y F Wang, C B Jiang and H B Xu . *Chin. Phys. Lett.* **2006**,23,1293
- [5] M Mohapatara, P Brajesh, V Chandan, S Anand, R P Das and H C Verma. *J. Magan. Mater* **2005**, 249,46
- [6] M. J Sugimoto. *Am. Ceram. Soc.* **1999**, 82 ,269
- [7] M Vuclic, W Jones and G D Moggride. *Clays Clay Miner.* **1997**,45, 803
- [8] Z Wu, X Wang and F Chin Wang. *Phy. Lett.* **2007**,24, 3249
- [9] C Busetto, G Del Piero, G Mamara , F Friiro and A.J Vaccar. *Catal.* **1984**,85, 260
- [10] X D Zhou, X Qi and F Li. *Mater. Mech. Engin.* **2009**,33, 88.
- [11] S Castro and M. J Gayoso. *Solid State Chem.* **1997**,134, 227.
- [12] K Mydeen, Y Yu and C. Chin Jin. *Phys. Lett.* **2008**, 25, 3177.
- [13] V R L Constantion and T J Pinnavaia. *Inorg. Chem.* **1998**,34,2086.
- [14] R M Taylor *clay Miner.* **1980**,15,369.
- [15] V Sepelak , D Baabe, F J Litterst and K D Backer **2000** *J. Appl. Phys.* 88,5884.
- [16] C. H. Lin, S. Q. Chen, *Chin. J. Mater.Sci.* **1983**, 15,31.
- [17] Z. Yue, Ji Zhou, L. Li, H. Zhang and Z. Gui, *J. Magn. Magan. Mater.* **2000**,208,55.
- [18] Ashwani Sharma, Pallavi, Sanjay Kumar, Sanjay Dahiya and Narender Budhiraja, *Advances in Applied Science Research*, **2013**, 41,124.
- [19] Ashwani Sharma, Pallavi, Sanjay Kumar and Sonia, *Archives of Applied Science Research*, **2012**, 4 (6),2557.
- [20] S.P. Chandran, M. Chaudhary, R Pasricha, A. Ahmad, M. Sastry, *Biotechnol. Prog.* **2006**,22,577.
- [21] B. D. Cullity, *Elements of X-ray Diffraction*, Adison-Wesley Publ. Co., London (**1967**)
- [22] V. R. K. Murthy and J. Sobhanadri, *Phys. Stat. Solidi. A.* **1971**, 36,133.
- [23] R.K. Selvan, C.O. Augustin,L.B. Berchmans, R. Sarawathi, *Mater.Res.Bull.* **2000**, 38,41
- [24] R. D. Waldron, *Phys. Rev.* **1955**,99,1727.
- [25] S.Yan, J. Geng, L. Yin, E. Zhou, *J. Magn.Magn.Mater.* **2001**,277,84 .
- [26] B.D.Cullity, *Introduction to Magnetic Materials*, Addison-Wesely Publishing Co.Inc.,Reading. MA.**1972**.
- [27] S. Chikazumi, *Physics of Magnetism*, Wiley, New York,**1959**.
- [28] A. Verma, D.C. Dube, *J. Am. Ceram.Soc.* **2005** 88,519.